The Reflectance of Silvery Fish Skins

Alex Malins[†]

January 5, 2009

[†]Bristol Centre for Complexity Sciences, University of Bristol, Bristol, BS8 1TS, UK

Supervision by Prof Noah Linden, Department of Mathematics, University of Bristol, and Prof Julian Partridge, School of Biological Sciences, University of Bristol.

Abstract

I investigate the optical properties of guanine cytoplasm bi-layer stacks common in fish skins, with the goal of understanding how the structure of the stacks is important in producing a silvery reflectance. A simple model for the optics of a guanine cytoplasm multilayer stack is used to predict the reflectivity across visible wavelengths of light. A method, termed "f-value" deviates measure, is devised to quantify the similarity of the reflectivity spectrum to a perfect silver mirror reflectivity spectrum. A MATLAB optimization routine is used to identify local solutions of stack layer thicknesses which minimize the f-value measure. I find that the larger the number of layers in the stack the easier it is to devise a guanine cytoplasm bi-layer stack with a spectrum similar to silver mirror uniform reflectance. I note that stacks with constant layer thicknesses, such as equal layer and quarter-wave stacks, are poor uniform reflectors compared to chirped and random layer thickness stacks and conclude that variation in layer thicknesses is important for silvery reflectance.

Contents

1 Introduction

Structural colours arise from the wavelength dependent refraction and reflexion of light passing through an optical structure. The highly reflective structures found in fish skin consist of alternating layers of high and low refractive index materials (guanine and cytoplasm) with thicknesses of same order of magnitude as the wavelengths of visible light. Camouflage as a survival strategy is highly developed in fish and is most commonly achieved by using multilayer stacks to give a colourful or silvery reflectance. Silver is commonly used to disguise the profile of the fish against the silvery surface of the water when viewed from beneath. This mechanism is of particular interest to engineers trying to manufacture perfect mirrors. An example of a multilayer stack from a ribbonfish is shown in figure 1.

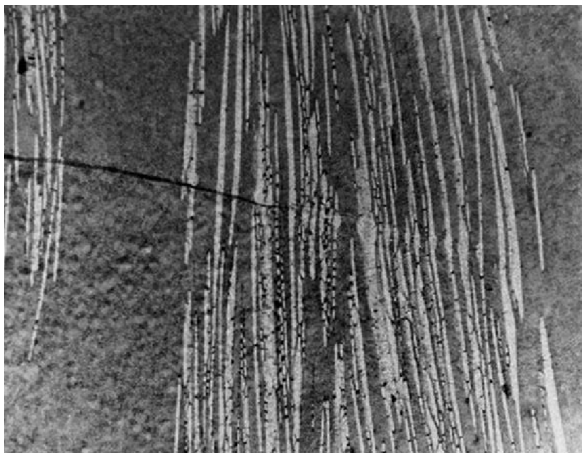

Figure 1: A transmission electron micrograph of the cross section of the skin of a ribbonfish showing bands of guanine crystals (light material) suspended in cytoplasm (dark material). Picture from McKenzie et al. [1995].

The origins of silvery colour in fish skins is mainly structural, not relying on pigments, dyes, or metallic elements. Usually there is a stack of parallel sided transparent layers with alternating refractive indices. The most common materials for the layers are guanine and cytoplasm. The former has a higher refractive index than the latter so the boundaries between the layers cause refraction and reflection of light. Reflected light from different layers interferes and colour is observed for wavelengths where the interference is constructive. Often the colour changes with the angle of incidence of the light because this changes the optical path lengths of the layers. The derivation of the model for the stacks is given in §2.1.

It is known that for a given number of layers and type of optical materials the highest reflectance is obtained when the optical thickness of the layers is a quarter-wavelength of light. However these quarter-wave stacks have narrow band reflectance spectra and are only suitable for coloured fish (Lythgoe et al. [1984]) and do not easily explain the silvery reflectance spectra common in fish.

I suggest a function, termed f-value, to measure the *likeness* of two reflectance spectra (§2.3). Specifically it is used to measure how close a model predicted spectrum of a multilayer stack is to the uniform 1 reflectance spectra of a silver mirror. With this ability, I attempt to find solutions of stack layer thicknesses with broad band reflectance spectra by using a MATLAB optimization algorithm to minimize this f-value (§2.4). The algorithm is initialized with a range of stack structures, including quarter-wave stacks, random stacks and equal layer stacks. The goal of this is to learn what factors are important in the layer structure for a broad band reflectance spectrum.

The theory of structural colour in multilayers has been studied since Huxley [1968] first derived a formula for the reflectance of a bi-component stack. Denton and Land [1971] noted the mechanism was used in fish to produce highly reflecting structures and suggested that fish were using quarter-wavelength layer thicknesses of guanine to produce the highest reflectivity. This solution was thought to be universal across all species until Lythgoe et al. [1984] suggested that quarter-wave stacks whilst adequate for coloured fish were not suitable for explaining the silvery reflectance seen in a wide variety of species. The idea of random stacks using optical localization to produce high reflectance was discussed by Yoo and Alfano [1989] and Martijn de Sterke and McPhedran [1993],

and McKenzie et al. [1995] wrote a paper claiming silvery fish skins could be explained entirely as random stacks, or chaotic reflectors.

2 Methods

2.1 The Optics of a Multilayer Stack

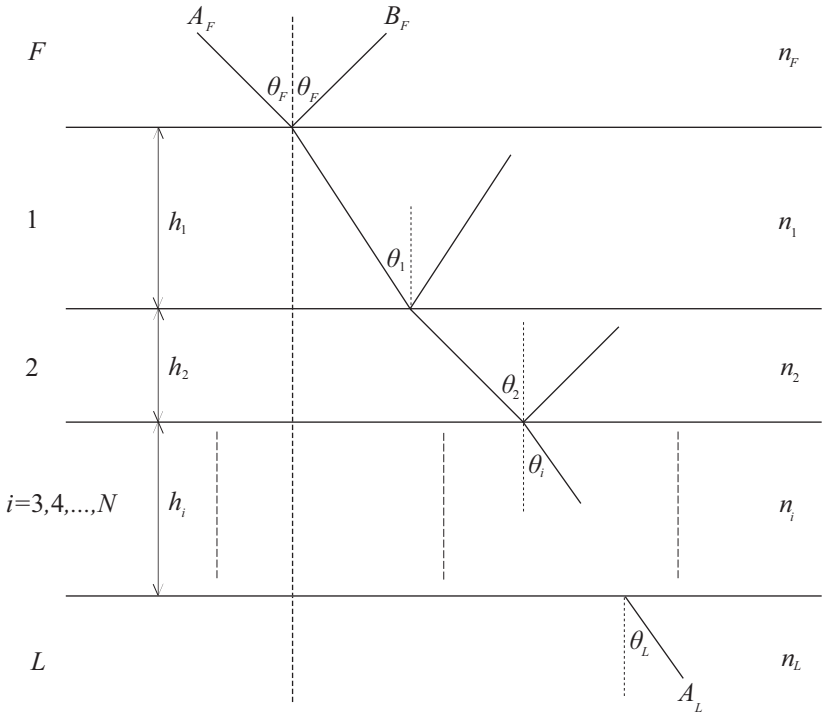

Figure 2: Diagrammatic illustration of the multilayer stack.

I model the guanine cytoplasm multilayer stacks in fish skin as *stratified medium*. This is a medium whose optical properties are constant throughout the planes perpendicular to a fixed direction. We consider a multilayer of N homogeneous dielectric films, denoted with index $i = 1, 2, .., N$, and stratified in the z-axis of a Cartesian coordinate system. The multilayer is bounded on each side by semi-infinite homogeneous media denoted by indices F and L respectively. All media are non-magnetic, or $\mu_i \equiv 1$, and have dielectric constant ε_i. Let n_F and n_L be the refractive indices of the first and the last semi-infinite media, and n_i and h_i be the refractive index and thickness of layer i in the multilayer. I define the coordinate system such that the stack extends from $z = 0$ to $z = \sum_{i=1}^{N} h_i = z_L$.

Imagine a plane, time-harmonic electromagnetic wave propagating through the medium. I consider the special case where the wave is linearly polarized with its magnetic vector perpendicular to the plane of incidence we speak of a *transverse electric wave* (TE); when it is linearly polarized with its magnetic vector perpendicular to the plane of incidence we speak of a *transverse magnetic wave* (TM) (any arbitrarily polarized wave may be resolved into a TE and a TM wave). These two waves are mutually independent. The incident wave has wave-number k and makes an angle θ_F to the z-axis. Wave-number k is constant throughout all media. The derivation of the reflectance of a multilayer stack follows the matrix method of Abelès [1950] given in Thin-film Optical Filters by Macleod [1986]. Standard results are cross-referenced with equation numbers in Principles of Optics by Born and Wolf [1999] where appropriate.

The angle the of the propagating wave in medium 1 is given by Snell's law[1]

[1] Born & Wolf §1.2 (10)+(13)

$$\frac{sin\theta_1}{sin\theta_F} = \frac{n_F}{n_1}, \tag{1}$$

i.e.

$$\theta_1 = sin^{-1}(\frac{n_F}{n_1} sin\theta_F). \tag{2}$$

The angle the transmitted wave makes to the z-axis in medium i by repeated application of Snell's law

$$\theta_i = sin^{-1}(\frac{n_{i-1}}{n_i} sin\theta_{i-1}). \tag{3}$$

The law of reflection states that light reflected at the boundaries of stack make the same angle to the (normal) z-axis as the incident light.

Without loss of generality I choose the plane of incidence to be the y, z-plane. For TE wave, $E_y = E_z = 0$ and Maxwell's equations show E_x, H_y and H_z are functions of y and z only. It follows that

$$\frac{\partial^2 E_x}{\partial y^2} + \frac{\partial^2 E_x}{\partial z^2} + n^2 k_0^2 E_x = \frac{d(ln\mu)}{dz}\frac{\partial E_x}{\partial z}, \tag{4}$$

and we try a solution of the form

$$E_x(y,z) = Y(y)U(z), \tag{5}$$

i.e. (4) becomes

$$\frac{1}{Y}\frac{d^2Y}{dy^2} = -\frac{1}{U}\frac{d^2U}{dz^2} - n^2k_0^2 + \frac{d(ln\mu)}{dz}\frac{1}{U}\frac{dU}{dz}. \tag{6}$$

By setting both sides of (6) to $k_0^2\alpha^2$, this solves as

$$E_x = U(z)e^{\imath(k\alpha y - \omega t)}. \tag{7}$$

Maxwell's equations also give H_y and H_z by expressions of the same form

$$H_y = V(z)e^{\imath(k\alpha y - \omega t)}, \tag{8}$$

$$H_z = W(z)e^{\imath(k\alpha y - \omega t)}. \tag{9}$$

U, V, and W are known as the amplitude functions and are in general complex functions of z. U and W are linearly dependent so in fact U and V are described by a pair of simultaneous first-order differential equations

$$\frac{dU}{dz} = \imath k\mu V, \tag{10}$$

$$\frac{dV}{dz} = \imath k(\varepsilon - \frac{\alpha^2}{\mu})U, \tag{11}$$

which reduce to two second-order linear differential equations

$$\frac{d^2U}{dz^2} - \frac{d(ln\mu)}{dz}\frac{dU}{dz} + k^2(n^2 - \alpha^2)U = 0, \tag{12}$$

$$\frac{d^2V}{dz^2} - \frac{d\left[ln(\varepsilon - \frac{\alpha^2}{\mu})\right]}{dz}\frac{dV}{dz} + k^2(n^2 - \alpha^2)V = 0. \tag{13}$$

There is an analogous pair of ODEs for the TM wave.

Since functions $U(z)$ and $V(z)$ each satisfy a second-order linear differential equation it follows that each may be expressed as a linear combination of two particular solutions U_1, U_2 and V_1, V_2. These are coupled as

$$\left.\begin{array}{l} \frac{dU_1}{dz} = \imath k\mu V_1, \\ \frac{dV_1}{dz} = \imath k(\varepsilon - \frac{\alpha^2}{\mu})U_1, \end{array}\right\} \quad \left.\begin{array}{l} \frac{dU_2}{dz} = \imath k\mu V_2, \\ \frac{dV_2}{dz} = \imath k(\varepsilon - \frac{\alpha^2}{\mu})U_2. \end{array}\right\} \tag{14}$$

From these relations it follows that

$$\frac{d}{dz}(U_1V_2 - U_2V_1) = 0, \tag{15}$$

and we choose convenient particular solutions

$$\left.\begin{array}{ll} U_1 = f(z), & U_2 = F(z), \\ V_1 = g(z), & V_2 = G(z), \end{array}\right\} \tag{16}$$

such that

$$f(0) = G(0) = 0, \quad F(0) = g(0) = 1. \tag{17}$$

Then the solutions with

$$U(0) = U_0, \quad V(0) = V_0, \tag{18}$$

may be expressed in the form

$$\left.\begin{array}{l} U = FU_0 + fV_0, \\ V = GU_0 + gV_0, \end{array}\right\} \tag{19}$$

or, in matrix notation,

$$\mathbf{Q} = \mathbf{N}\mathbf{Q_0}, \tag{20}$$

where

$$\mathbf{Q} = \begin{bmatrix} U(z) \\ V(z) \end{bmatrix}, \quad \mathbf{Q_0} = \begin{bmatrix} U_0 \\ V_0 \end{bmatrix}, \quad \mathbf{N} = \begin{bmatrix} F(z) & f(z) \\ G(z) & g(z) \end{bmatrix}. \tag{21}$$

It is normally the case that U_0 and V_0 are expressed as functions of $U(z)$ and $V(z)$,

$$\mathbf{Q_0} = \mathbf{M}\mathbf{Q}, \tag{22}$$

where $|\mathbf{M}| \equiv |\mathbf{N}| \equiv 1$ and

$$\mathbf{M} = \mathbf{N}^{-1} = \begin{bmatrix} g(z) & -f(z) \\ -G(z) & F(z) \end{bmatrix}. \tag{23}$$

$\mathbf{M}$ is the characteristic matrix of a stratified medium and it relates the x and y-components of the electric (or magnetic) vectors in the $z = 0$ plane to the components in an arbitrary $x, y-$plane.

The characteristic matrix for a plane wave propagating through a homogeneous dielectric film is specified in Born & Wolf[2]. For the TE wave in layer i this is[3]

$$\mathbf{M_i}(h_i) \quad = \quad \begin{bmatrix} \cos(kn_ih_i\cos\theta_i) & -\frac{\imath}{n_i\cos\theta_i}\sin(kn_ih_i\cos\theta_i) \\ -\imath n_i\cos\theta_i\sin(kn_ih_i\cos\theta_i) & \cos(kn_ih_i\cos\theta_i) \end{bmatrix}, \tag{24}$$

The characteristic matrices for the TM wave are slightly different, and are obtained by replacing the first n_i in the off diagonal components of the matrices by $\frac{1}{n_i}$ [4].

For our multilayer stratified media we obtain the characteristic matrix by[5]

[2] Born & Wolf §1.6.1 & §1.6.2
[3] Born & Wolf §1.6.2 (39)
[4] Born & Wolf §1.6.2 (40)
[5] Born & Wolf §1.6.2 (41)

$$\mathbf{M}(z_L) = \mathbf{M_1}(h_1)\mathbf{M_2}(h_2)\mathbf{M_3}(h_3)...\mathbf{M_{N-1}}(h_{N-1})\mathbf{M_N}(h_N) \tag{25}$$

$$= \begin{bmatrix} m_{11} & m_{12} \\ m_{21} & m_{22} \end{bmatrix}. \tag{26}$$

Let A_F, B_F denote the amplitudes of the incoming and outgoing waves for the first semi-infinite medium, and A_L, B_L denote the amplitudes of the outgoing and incoming waves for the last semi-infinite medium. It is reasonable to assume $B_L = 0$, as physically this means a fish does not radiate light internally through its skin. Using

$$\mathbf{H} = \sqrt{\frac{\varepsilon}{\mu}}\mathbf{s} \times \mathbf{E}, \tag{27}$$

the following relations for a TE wave are derived

$$\left.\begin{array}{cc} U_0 = A_F + B_F, & U(z_L) = A_L, \\ V_0 = n_F \cos\theta_F (A_F - B_F), & V(z_L) = n_L \cos\theta_L A_L. \end{array}\right\} \tag{28}$$

Using (22) we see that

$$\left.\begin{array}{c} A_F + B_F = (m_{11} + m_{12} n_L \cos\theta_0) A_L, \\ n_F \cos\theta_F (A_F - B_F) = (m_{21} + m_{22} n_L \cos\theta_L) A_L. \end{array}\right\} \tag{29}$$

Set $A_L = 1$ and solve simultaneously for A_F and B_F. We obtain

$$A_F = \frac{1}{2}(m_{11} + m_{12} n_L \cos\theta_L + \frac{m_{21} + m_{22} n_L \cos\theta_L}{n_F \cos\theta_F}) \tag{30}$$

$$B_F = \frac{1}{2}(m_{11} + m_{12} n_L \cos\theta_L - \frac{m_{21} + m_{22} n_L \cos\theta_L}{n_F \cos\theta_F}) \tag{31}$$

The *reflectivity* and the *transmissivity* are

$$\mathcal{R}_{TE} = \frac{|B_F|^2}{|A_F|^2}, \tag{32}$$

$$\mathcal{T}_{TE} = \frac{n_L \cos\theta_L}{n_F \cos\theta_F} \frac{1}{|A_F|^2}. \tag{33}$$

To obtain the reflectivity and transmissivity of the TM wave replace all the n_i by $\frac{1}{n_i}$ in (30), (31), (32) and (33).

As the reflected and transmitted plane polarized waves are time-harmonic sinusoidal, it is possible to take their average to give the reflectivity and transmissivity of incident unpolarized light. The average of a time-harmonic sinusoidal function

$$\int_{-a}^{a} \sin^2(\omega t + \delta) dt = \frac{1}{2}, \tag{34}$$

which means the unpolarized reflectivity and transmissivity are

$$\mathcal{R} = \frac{1}{2}(\mathcal{R}_{TE} + \mathcal{R}_{TM}), \tag{35}$$

$$\mathcal{T} = \frac{1}{2}(\mathcal{T}_{TE} + \mathcal{T}_{TM}). \tag{36}$$

It is possible to show that the power of the incident wave is equal to the sum of the power of the wave transmitted through the stack and the power of the reflected wave and the system conserves energy. The following

relation, for a *TE* wave, provides a useful check that the implementation of the solution in MATLAB does indeed obey the law of energy conservation

$$n_F \cos\theta_F(|A_F|^2 - |B_F|^2) - n_L \cos\theta_L = 0, \tag{37}$$

or perhaps more simply,

$$\mathcal{R}_{TE} + \mathcal{T}_{TE} = 1. \tag{38}$$

From here on I mainly refer to the reflectivity of a multilayer stack, as it is trivial to infer the transmissivity from this quantity.

2.2 MATLAB Implementation

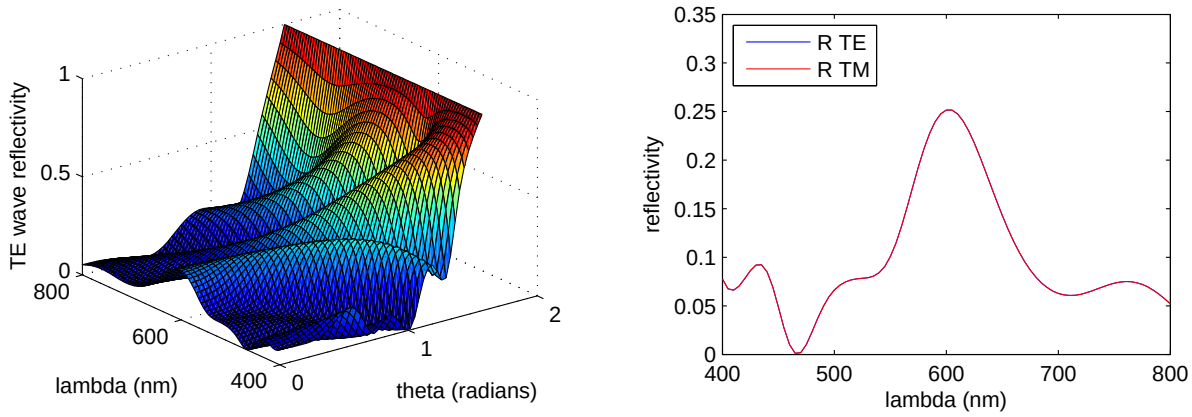

(a) Reflectivity as a function of wavelength and angle of incidence.

(b) Reflectivity of normally incident visible light. Both *TE* and *TM* reflectivity coincide.

Figure 3: The *TE*-component reflected from a multilayer stack as a function of wavelength and angle of incidence of incident light for a four layer stack with random thicknesses and refractive indices.

The preceding section derives analytic formulae for the reflectance and transmittance of a plane wave incident on a multilayer stack with infinite and parallel plane layers. The solution is only valid for isotropic and non-magnetic media with both these assumptions valid for cytoplasm. It is, however, known that guanine is not isotropic due to its crystal structure.

The reflectivity and transmissivity are functions of the following variables:

1. N- the number of layers in the stack,
2. $\{n_i\}$, n_F, n_L - the refractive indices of the layers, and the first and last semi-infinite media ($i \in 1, 2, \ldots, N$),
3. $\{h_i\}$ - the thicknesses of the layers ($i \in 1, 2, \ldots, N$),
4. k (or λ) - the wave-number (or wavelength) of the incident plane wave,
5. θ_F - the angle of incidence of the incident plane wave,
6. and the polarization of the incident plane wave.

I use MATLAB to calculate the reflectivity and transmissivity for both *TE* and *TM* wave as a function of these parameters with code `basicmodel.m` (§B.1). Sample spectra for a four layer stack with random layer thicknesses and refractive indices are shown in fig 3.

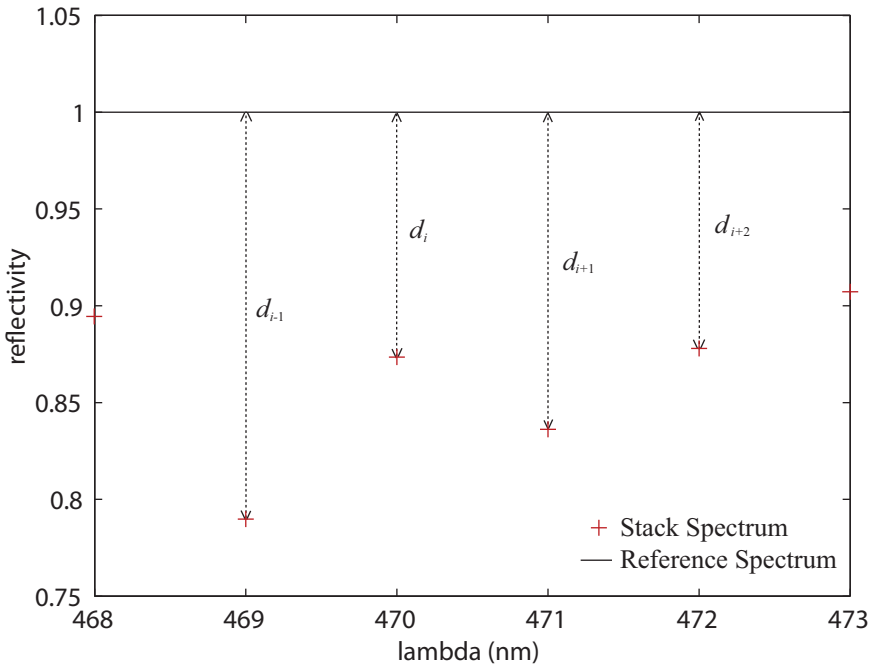

Figure 4: Diagram of square deviates from spectra

2.3 "f-value" Spectral Similarity Measure

A simple method is devised to quantity the similarity of a predicted spectrum to any reference spectrum. Define a reference reflectivity spectrum $\mathcal{R}_{ref} = \mathcal{R}(\lambda, \theta)$ as a function of incident light with λ wavelength and θ angle. A stack, defined by parameters N, $\{n_i\}$, n_F, n_L and $\{h_i\}$ for $i \in 1, 2, \ldots, N$, has calculated reflectivity in the form $\mathcal{R}_{stack} = \mathcal{R}(\{\lambda_l\}, \{\theta_j\})$ where wave-numbers are discrete points λ_l, $l \in \mathcal{L}$ as are angles of incidence θ_j, $j \in \mathcal{J}$. For a discrete point on the spectrum, the deviation with moment m is

$$d_{l,j}^m = (\mathcal{R}_{ref}(\lambda_l, \theta_j) - \mathcal{R}_{stack}(\lambda_l, \theta_j))^m. \tag{39}$$

Moments $m \in \{2, 4, 6, \ldots\}$. The "f-value" with moment m is used to measure the deviation of the stack spectrum from the reference spectrum

$$f_m = \frac{\sum_{l \in \mathcal{L},\, j \in \mathcal{J}} d_{l,j}^m}{|\mathcal{L}|\,|\mathcal{J}|}. \tag{40}$$

An important consequence to note is that $f_m \in [0, 1]$ always.

The f-value is always greater than zero and defines a surface in a $(|\mathcal{L}| + |\mathcal{J}| + 1)$-dimensional space. The global minima of the surface is the optimal stack such that its spectrum is closest to the reference spectrum using the deviation measure (39) defined. Example code which calculates the square f-value (moment 2) is given in `stacksquaredresiduals.m` (B.2).

2.4 MATLAB Optimization Routine

I employ a numerical algorithm of the MATLAB optimization toolbox to search f-value space for local minima. The local minima correspond to multilayer stacks parametrized to produce a spectrum as a best fit to the reference spectrum. To model the reflectance of fish skin I consider the a multilayer stack of guanine crystals suspended in

cytoplasm. This defines both $n_F = n_L = 1.365$, i.e. the first and last semi-infinite media are cytoplasm, and

$$n_i = \begin{cases} n_G = 1.84 & \text{odd } i \\ n_C = 1.365 & \text{even } i \end{cases}.$$

For simplicity only the case of normal incidence light is considered and incident light of visible wavelengths (300nm to 800nm or 400nm to 800nm depending on N). This means f-value moment m reduces to a function of the layer thicknesses only, i.e. $f_m = f_m(\{h_i\})$. The number of layers and their thicknesses are the parameters which fish biology has control. The reference spectrum I use has maximum reflectivity for all visible wavelengths

$$\mathcal{R}_{ref} = 1, \ \forall \lambda_i. \tag{41}$$

This spectrum corresponds to a perfect silver mirror, or white if the surface is Lambedian, and is a good approximation for the spectrum of silvery fish skins.

The optimization algorithm used is `fminunc.m` unconstrained nonlinear minimization. The algorithm works to minimized the instantaneous f-value of a stack by controlling the square root of the thicknesses of the first $N-1$ layers, i.e. $\{\sqrt{h_i}\}$. This enforces that all thicknesses are non-negative without having to use a slower constrained optimization routine. I choose N even such that the last layer of the stack is cytoplasm, and its thickness of the last layer h_N is determined by a large parameter defining the maximum thickness of the multilayer stack. The thickness of this last layer of cytoplasm does not affect the spectrum of the stack, as in effect it becomes part of the last semi-infinite cytoplasm layer. Defining the routine this way allows me to ensure the total stack thickness does not grow to an unphysical size during the optimization routine.

`fminunc.m` uses the BFGS Quasi-Newton method with a cubic line search procedure. It approximates the Hessian of the f-value function and updates this approximation using the BFGS method. `fminunc.m` is an entirely deterministic routine and it might only converge converge to local solutions (i.e. local minima of the f-value surface) (Broyden [1970], Fletcher [1980]). All algorithm settings are default bar a increase in the 'maximum number of function evalutions' (to $10^4 * \text{numberOfVariables}$), increase in the 'maximum number of iterations' (to 10^5) and a decrease in 'X tolerence' (to 10^{-5}). These parameters are chosen to ensure convergence to solution and on a feasible timescale (optimization runs lasting 5 days maximum). The optimization routine must be initialized from a starting configuration of a set of layer thicknesses which one can choose at will.

3 Results

3.1 Minimization Algorithm Parameters

In the following results I always use a perfect silver mirror unity reference spectrum (equation 41). Spectra are evaluated for $N = 50$ or 200 layers, where there are $\frac{N}{2}$ guanine and $\frac{N}{2} - 1$ cytoplasm optically significant layers. The reflectivity of the stack is calculated at 1nm intervals in wavelengths 400nm to 800nm for $N = 50$, and 300nm to 800nm for $N = 200$. All other settings are as section §2.4.

The initial thicknesses of the layers of the stack are chosen in five ways:

1. randomly so the total thickness of the $N - 1$ are uniformly distributed in the range $[0, h_T]$. For 50 layer random stacks $h_T = 100\mu$m, and for 200 layer random stacks $h_T = 200\mu$m (§3.2+§3.3),
2. 200 layer stacks with constant layer thickness (§3.4),
3. quarter-wave stack optimized for wavelength $\bar{\lambda}$, i.e. $h_G = \frac{\bar{\lambda}}{4n_G}$, $h_C = \frac{\bar{\lambda}}{4n_C}$ (200 layers in §3.5 and 50 layers in §A.2),
4. 200 layer stacks with guanine layer thicknesses optimized for wavelength $\bar{\lambda}$ ($h_G = \frac{\bar{\lambda}}{4n_G}$) and cytoplasm layer thicknesses chosen randomly in $[0, 1]$ (§3.7),
5. as chirped stacks with systematically changing thicknesses, e.g. increasing linearly from 0.1nm to 2nm (§3.6).

3.2 Random Stacks Optimizing Square Deviates

Number of Layers, N	50		200	
Number of Stacks Sampled	105		103	
	Input	Output	Input	Output
Mean Stack Thickness, $h^{in/out}{}_T$ (μm)	48.67	48.92	114.50	114.56
Mean f-value, $f_2^{in/out}$	0.268	0.109	0.0363	0.00767
Standard Deviation of f-value, $\sigma_{f_2^{in/out}}$	0.0598	0.0367	0.00589	0.0115
Lowest f-value, $\min\{f_2^{in/out}\}$	0.204	0.00853	0.0216	0.0000110
Sample Mean Reflectivity	0.561	0.718	0.913	0.967
Sample Mean S.D. of Reflectivity	0.275	0.171	0.167	0.0767

Table 1: Results for second moment random stack optimization runs.

For both the 50 and 200 layer cases I sample over 100 random random stacks with second moment optimization runs and the results are listed in table 1. The first general result I note is that as the number of layers in the stack increases the mean f-value, or total reflectivity, of the stack increases. The optics of bi-layer stacks implies this a result, and is confirmed by the decrease in f-value of the stacks after optimization. The optimization routine attempts to improve the silvery reflectance (as measured by f-value) of a multilayer stack, but the results demonstrate that a randomly generated 200 layer stack is likely to have lower f-value than an optimized 50 layer random stack (200 layer $\bar{f_2^{in}}$ is lower than 50 layer $\bar{f_2^{out}}$). An obvious method for a fish to increase its skin reflectivity is to increase the number of guanine-cytoplasm bi-layers in its skin.

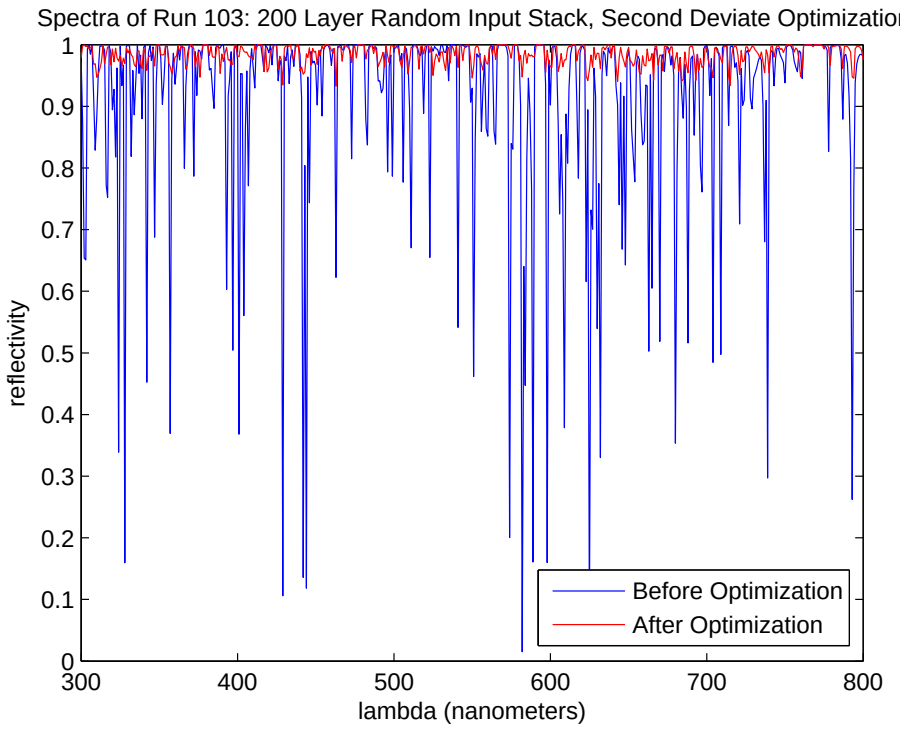

Figure 5: Input and output stack spectra of optimization run 103. An input 200 layer stack with random layer thicknesses has spectrum shown with the blue line before the optimization routine. On completion the output stack has a spectrum shown in red. It is clear the red line is a closer match to a unity spectrum of a silver mirror. $f_2^{in} = 0.0354,\ f_2^{out} = 0.000489$.

Figure 5 shows the spectra of a random 200 layer stack before and after optimization; the blue line is the spectrum of the initial stack with random layer thicknesses and the red line is the spectrum of the stack produced by the optimization routine. It is clear the output red spectrum is a better approximation to the unity silver mirror spectrum than the input blue spectrum.. A simple method to measure the reflectivity of a stack is to consider a mean reflectivity across the whole spectrum. This tells us the absolute proportion of the incident light which is reflected and is perhaps more intuitive than f-value, but drops the detail of the spectrum and hence the colour of the returning light itself. For example run 103 of the 200 layer random stacks shown in figure 5 has a mean input stack reflectivity of around 0.91 or 91%, whilst the output spectrum has mean reflectivity of nearly 0.98 or 98%. There are also far fewer "low reflectivity spikes", characteristic of the blue spectrum, in the output red spectrum; the standard deviation of the reflectivity for the input stack is 17% compared with 1.5% for the output stack. The spikes of low reflectivity for particular wavelengths cause the reflection to be more colourful than silver. The fourth moment f-value optimization routine is designed to penalize these low reflectivity spikes in order to give a flatter spectrum and more silvery reflection.

Figure 5 is typical of the 50 and 200 random layer second moment optimization runs. Over all the runs, the mean reflectivity at a given wavelength is given in the second to last row of table 1 and the mean standard deviation of spectral reflectivity of all runs in the last row of that table. For both the 50 and 200 layer optimization routines the mean reflectivity increases resulting in an improvement wavelength of around 15% and 5% respectively, and the standard deviation decreases indicating the reflectivities are less varied after optimization.

Discussing absolute reflectivities becomes inappropriate when the desired reflectivity spectrum is not unity silver mirror. It is for this reason the more general f-value measure was suggested. The mean second moment f-value of the 50 layer stacks decreases by a factor greater than 2 on optimization, and likewise the f-value of the 200 layer random stacks decreases by a factor of almost 5 when optimized. This is reassuring in that it shows the optimization routine does indeed improve the silvery reflectance of a stack according to the measure I suggest.

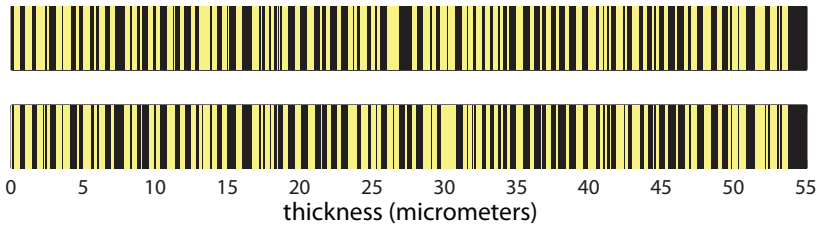

Figure 6: A diagram of 200 layer stack run 103 before and after the second moment optimization routine. The yellow layers are guanine and the black corresponds to cytoplasm, with the last black region at the right of the figure being the semi-infinite cytoplasm. Both before and after figures are to the same scale. $f_2^{in} = 0.0354$, $f_2^{out} = 0.000489$.

The stacks with lowest f-value match the silver mirror spectrum closely and are considered as "best performing". Both sample mean f-values and sample minimum f-values are listed in table 1. There is a general trend in the results showing that the stacks with smaller mean layer thickness have lower f-values.

Drawing the multilayer stack to scale enables one to examine how the thickness of the layers define the stack structure. Figure 6 shows a to-scale render of a 200 layer stack before and after optimization (run 103 of figure 5). The yellow regions represent guanine layers and the black areas represent cytoplasm. Firstly it is clear that the total thickness of the stack has not changed appreciably with the optimization, and this is the case for all the random stack optimization runs (both for 50 and 200 layer stacks). Table 1 gives the mean input and output thicknesses of the stacks, and these quantities only differ by slight amounts. This phenomena highlights a serious limitation of the optimization routine: it will in all probability fail to find the mathematical solution of the best silvery reflective stack if does not explore the space of stack thicknesses.

The way the optimization routine is defined means the total stack thickness is a free variable, and in some of the later sections (such as quarter-wave stacks) the routine does change the total stack thicknesses appreciably. It is a curious result that the routine does not do so for the random initial stacks and the most likely explanation for this failure is that the routine hones in on a local minima of the f-value surface and terminates there. More investigation is needed into the parametrization and set up of the optimization routine to try and solve this issue. In theory it is also possible to use other methods such as grid sampling and basin hopping to find the global minimum(a) of the f-value surface and hence the optimal solution(s) and for more comment on this see the extensions section (§5).

From the renders of figure 6 it is also clear that the layer structure of the stack does not change markedly after optimization. Both the input stack and the output stack have a very similar guanine-cytoplasm bi-layer structure, with the renders bearing a strong resemblance to two similar bar-codes - layers are in roughly the same position in both stacks and there is only a slight variation in layer thicknesses at a local level. Histograms of the distribution of the guanine and cytoplasm layer thicknesses allow us to see more clearly any changes in layer thicknesses on optimization. Figure 7 shows the distributions of a 200 layer stack, with only vary slightly before and after optimization. The distributions of figure 7 are typical of all the random stack optimizations (both 50 and 200 layers), with only a slight change in distribution being seen.

The fact that the optimization routine fails to appreciably change the total stack thickness and the distribution of the layer thicknesses raises the following points. Firstly that the f-value landscape contains a large number of local minima (I find one for each optimization run). The proportion of these minima that are accounted for by symmetries is not clear. The optimization routine demonstrates that changing the distribution of the layer thicknesses by only a slight amount can lead to a significant improvement in the silver appearance of the stack. In fact a quarter of 200 layer random stack optimizations lead to a factor 100 decrease in f-value, which is a very significant improvement. Although such radical decreases in f-value were not seen for the 50 layer random stacks, nearly all optimizations halved the f-value of the stack or more. Therefore it appears that the reflectivity of a stack is highly sensitive to a small change in a layer thickness. It is also true that there are a large number of almost degenerate solutions for a given number of layers, and to ensure a higher reflectivity it is simplest to increase the number of layers in the stack.

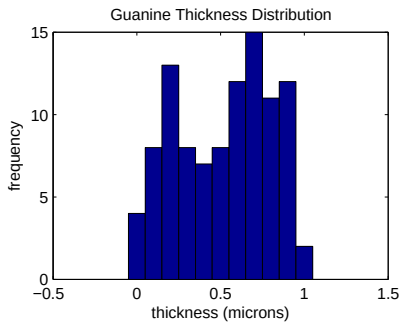

(a) Input random thickness distribution of guanine layers.

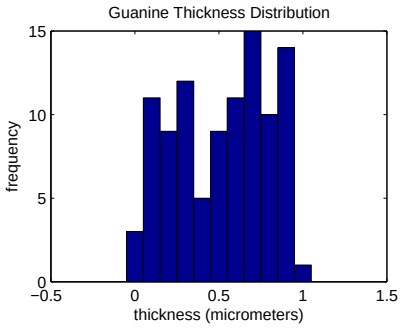

(b) Distribution of guanine thicknesses after optimization. There is only a slight change when compared to the input distribution.

Figure 7: Histograms of thicknesses of 100 guanine layers before and after second moment optimization. In general for the random stack optimizations, the thickness distributions only distort slightly after optimization - for both guanine and cytoplasm layers. This is most likely a consequence of the routine terminating on a local minima of the f-value surface. There is no general trend for the change of the distributions.

3.3 Random Stacks Optimizing Fourth Deviates

Number of Layers, N	50		200	
Number of Random Input Stacks	104		110	
	Input	Output	Input	Output
Mean Stack Thickness, $h_T^{in/out}$ (μm)	55.08	55.24	108.02	108.03
Mean f-value, $f_4^{in/out}$	0.153	0.0357	0.0164	0.00453
Standard Deviation of f-value, $\sigma_{f_4^{in/out}}$	0.0656	0.0108	0.00421	0.00486
Lowest f-value, $\min\{f_4^{in/out}\}$	0.110	0.00337	0.00783	0.00000119
Sample Mean Reflectivity	0.558	0.676	0.913	0.942
Sample Mean S.D. of Reflectivity	0.277	0.178	0.168	0.111

Table 2: Results for random stack fourth deviate optimization runs.

The conclusions drawn from random stack second moment f-value optimizations (§3.2) generally apply to random stack optimizations using a fourth moment f-value function. More precisely:

1. 50 layer output stacks are have lower f-values than 200 layer random input stacks, so in general the more layers the better the silver reflectance of the stack.
2. The spectral mean reflectivity increases and the spectral standard deviation of reflectivity decreases for all sample runs.
3. The $N = 200$ layer optimizations see a greater decrease in fourth moment f-value than the 50 layer optimizations in terms of factor of reduction, but not in terms of magnitude of reduction.
4. In general the thinner the layers of the stack, the lower the f-value.
5. Each optimization run terminates at a local minima of the fourth moment f-value landscape, with only a fractional change in stack thickness and layer thickness distributions.

The premise behind the fourth moment f-value measure is that reflectivities far from unity at a given wavelength are penalized. The fourth moment f-value optimization should result in spectra with less outlying low reflectivity

points than the second moment optimized stacks, perhaps at the expense of overall mean reflectivity. Although a direct comparison is not strictly fair as the square and fourth optimization runs start with different random stacks, the square moment output spectra have average reflectivity of 0.967 whereas the fourth moment output spectra have a 0.942 reflectivity (both figures quoted for 200 layer stacks). Therefore the square deviate optimization produces stacks with higher mean reflectivities, as expected.

The square moment output stacks have slightly lower standard deviations of reflectivity on average for the 200 layer stacks, and an insignificant difference for the 50 layer stacks. This indicates there is slightly less variation in reflectivities of the output spectra than the fourth moment output spectra. The lower standard deviation does not necessarily imply fewer "low reflectivity spikes" in the spectrum however. On plotting the spectra there is no discernable difference in numbers of low reflectivity outliers between the second and fourth moment output stacks. Therefore it is difficult to tell if the fourth moment optimization run is an improvement in this regard without analyzing the statistics of the outliers further. Note it is not possible to quantitatively compare second moment f_2 and fourth moment f_4 f-values directly as the units are different.

3.4 Equal 200 Layer Stacks Optimizing Square Deviates

Input Layer Thickness, h^{in} (μm)	0.5	1	1.5	2	3
Input Total Thickness, h_T^{in} (μm)	99.5	199	298.5	398	597
Input f-value, f_2^{in}	0.771	0.764	0.774	0.765	0.769
Output f-value, f_2^{out}	0.000169	0.000209	0.000327	0.0884	0.150
Output Total Thickness, h_T^{out} (μm)	82.43	170.98	279.22	431.90	606.51
Mean Output Layer Thickness, h^{out} (μm)	0.414	0.859	1.40	2.17	3.05
S.D. of Output Layer Thicknesses, $\sigma_{h_i^{out}}$ (μm)	0.129	0.104	0.298	0.153	0.0373

Table 3: Results for second moment equal layer thickness 200 layer stack optimization runs.

In this section all the guanine and cytoplasm layers in the input stacks have constant thicknesses. The layer thicknesses are given in the heading of table 3, there are 200 layers in total and the second moment optimization routine is employed. All five equal-layer thickness stacks studied have a poor reflectivity when compared to the random stacks; their second moment f-values are above 0.75, whereas the highest f-value for a (input) random 200 layer stack f_2^{in} is slightly less than 0.05 and the mean is 0.0363. Therefore the constant layer stacks are poor silver mirror solutions.

Upon optimization there is a marked improvement in uniform reflectivity for the stacks with initial layer thickness less than 2μm, as the f-value decreases by a factor of at least 2000 to an output around 0.0002. This makes them better uniform reflectors than most of the optimized 200 layer random stacks, where $\bar{f_2^{out}} = 0.00767$. The thicker layer equal stacks do not perform as well after optimization, perhaps as layers greater than 2μm are not optically effective.

In all the equal layer runs the thickness of the stack changes much more than the fractional changes witnessed with the random stack optimizations, with some optimization seeing a 10% change in the total stack thickness. The layer thickness distributions still only change slightly, with the output thicknesses clustered around the input thickness with a standard deviation $\sim 0.1\mu$m. Again it appears the optimization algorithm is terminating in a local minima of the f-value surface.

The variation in output layer thicknesses is seen for the 0.5μm equal layer stack in figure 8. A tentative conclusion may be drawn that the single layer thickness stacks are not as good reflectors as random layer stacks, by virtue of the high f-values of the input stacks. More single layer thickness stacks would have to be sampled to confirm this however.

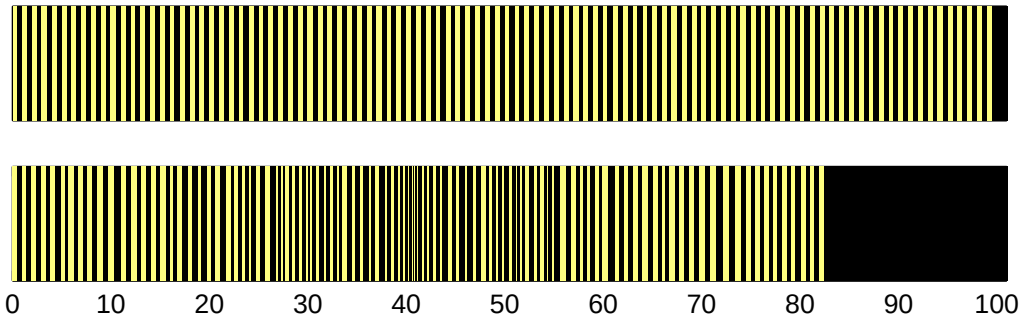

Figure 8: To-scale diagram of the 0.5μm equal layer wave stack before and after optimization. Variability in the layer thicknesses is introduced by the optimization routine to improve the f-value of the stack. Thickness are in micrometers and colours as figure 6. $f_2^{in} = 0.771$, $f_2^{out} = 0.000169$.

3.5 Quarter Wave, 200 Layer, Stacks Optimizing Square Deviates

Wavelength (nm)	300	350	400	450	500	550
Input Total Thickness, h^{in} (μm)	9.52	11.10	12.69	14.27	15.86	17.45
Input Guanine, h_G^{in} (μm)	0.0408	0.0476	0.0543	0.0611	0.0679	0.0747
Input Cytoplasm, h_C^{in} (μm)	0.0549	0.0641	0.0733	0.0824	0.0916	0.101
Input f-value, f_2^{in}	0.848	0.748	0.708	0.674	0.647	0.625
Output f-value, f_2^{out}	0.000165	0.0948	0.0555	0.000372	0.0801	0.000159
Output Total Thickness, h^{out} (μm)	51.33	394.48	70.05	18.67	518.93	57.35
Output Mean Guanine, h_G^{out} (μm)	0.278	2.24	0.418	0.0894	2.93	0.291
Output S.D. Guanine, $\sigma_{h_G^{out}}$ (μm)	0.374	3.28	0.658	0.120	3.45	0.444
Output Mean Cytoplasm, h_C^{out} (μm)	0.238	1.72	0.285	0.0983	2.28	0.286
Output S.D. Cytoplasm, $\sigma_{h_C^{out}}$ (μm)	0.296	2.264	0.505	0.129	2.52	0.399

Wavelength (nm)	600	650	700	750	800
Input Total Thickness, h^{in} (μm)	19.03	20.62	22.20	23.79	25.38
Input Guanine, h_G^{in} (μm)	0.0815	0.0883	0.0951	0.102	0.109
Input Cytoplasm, h_C^{in} (μm)	0.110	0.119	0.128	0.137	0.146
Input f-value, f_2^{in}	0.609	0.597	0.612	0.677	0.759
Output f-value, f_2^{out}	0.101	0.00000339	0.102	0.0327	0.00000850
Output Total Thickness, h^{out} (μm)	108.30	22.96	49.24	89.55	18.10
Output Mean Guanine, h_G^{out} (μm)	0.555	0.108	0.236	0.455	0.0710
Output S.D. Guanine, $\sigma_{h_G^{out}}$ (μm)	0.371	0.0655	0.0889	0.241	0.0255
Output Mean Cytoplasm, h_C^{out} (μm)	0.533	0.123	0.259	0.445	0.111
Output S.D. Cytoplasm, $\sigma_{h_C^{out}}$ (μm)	0.313	0.0648	0.0856	0.212	0.0446

Table 4: Results for second moment quarter-wave 200 layer stack optimization runs.

It is attractive to study quarter wave stacks as they are the optimal solution for the maximum reflectance at a given wavelength. There is a large bank of information about quarter-wave stacks (and their anti-reflective siblings the half-wave stacks) in optics literature and in the past it has been predicted that combinations of different wavelength quarter-wave stacks might be a good solution for a uniform silver mirror reflector (Denton and Nicol [1965]). However McKenzie et al. [1995] state this is not an appropriate structure for the reflectance of

silvery fish skins.

In this section I take 11 quarter-wave stacks, calibrated for wavelengths over the visible light spectrum, and input them into to the second moment optimization routine. The results are given in table 4. I first note that the input stacks are shown to be poor uniform reflectors with high f_2^{in} values (> 0.5). This is because reflectivities at wavelengths other than the calibrated one for the stack are generally poor (or even zero).

Upon optimization the majority of the quarter-wave stacks (specifically 300, 350, 400, 500, 550, 600, 700, 750nm) increase in thickness dramatically - for example the 550nm stack grows from 17.45μm to 57.35μm thick. The increase in stack thickness is a departure from what is witnessed for the random stack optimizations where stack thicknesses change only fractionally. With 300 and 550nm quarter-wave stacks as notable exceptions, the thickened quarter-wave stacks see a decrease in f-value by a factor 10, resulting in $f_2^{out} \simeq 0.05$ which is still greater than $\bar{f_2^{in}} \simeq 0.04$ for the 200 layer random stacks. The large increase in stack thickness coupled with the relatively large f_2^{out} values of some quarter-wave stacks may indicate optimization algorithm performance issues. Renders of the 700nm stack before and after optimization are shown in figure 9a and clearly indicate the growth in stack thickness.

The output stacks with similar thickness to the input quarter wave stack (450, 650, 800nm) see a many orders of magnitude reduction in f-value. The 650nm output stack has the lowest f-value of all stacks presented in this thesis, with $f_2^{out} = 3.39 \times 10^{-6}$ being a remarkably good approximation to the perfect silver mirror (figure 9b). These three quarter-wave stacks and the exceptions noted in the preceding paragraph (300 and 550nm stacks) become good uniform reflectors on optimization.

In all quarter-wave cases the output standard deviation of guanine and cytoplasm layer thicknesses is of the order of tenths of micrometers. This goes some way to demonstrate that variation in optical thicknesses of layers is needed for uniform reflectance. The histogram of cytoplasm layer thickness for the 550nm quarter-wave stack before and after optimization in figure 10 displays more clearly than the renders of figure 9 how the optimization algorithm improves f-value by introducing variation into layer thicknesses.

These results from the optimization algorithm are somewhat curious and it may be dangerous to speculate too deeply about their meanings. What is certainly true is that that the quarter-wave stacks are not good uniform reflectors, for the λ quarter-wave stack is also the $\frac{\lambda}{2}$ anti-reflective half-wave stack. For all quarter-wave stacks examined there is a significant standard deviation in the guanine and cytoplasm thicknesses of the output (in general of the same order as the initial thickness respectively). This appears to indicate, along with the results for the equal layer wave-stacks of §3.4 that it is a variation in thicknesses that is important in producing a silver reflectivity. Appendix §A.1 includes renders of all the quarter-wave stack optimizations not displayed here.

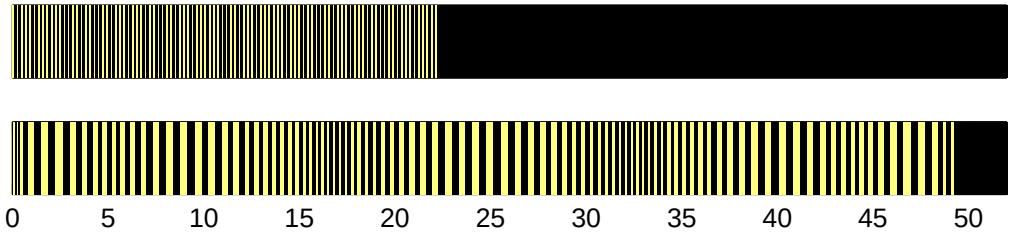

(a) A 700nm quarter wave stack initially $\sim 24\mu$m thick grows to almost 50μm on optimization. The second deviate f-value f_2 only decreases from 0.612 to 0.102 and both these values are greater than any of the random input stacks f-values.

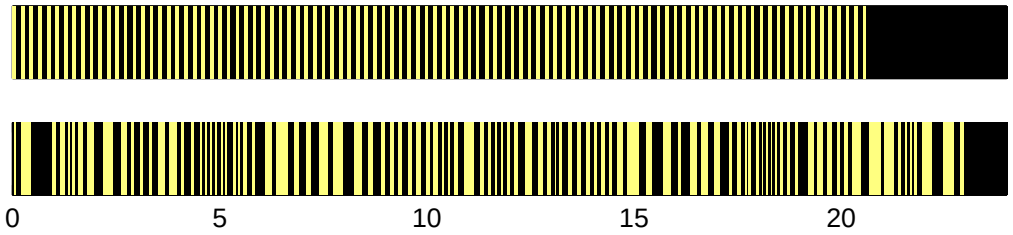

(b) Diagram of the 650nm multilayer stack before and after optimization second moment f-value optimization. The total stack thickness has not changed much and the f_2 value decreases from 0.597 to 0.00000339. The 650nm quarter-wave output stack is the best silver mirror reflector in this thesis using the second deviate measure.

Figure 9: To-scale diagrams of the 700nm (9a) and the 650nm (9b) quarter-wave stacks before and after optimization. Note how the 700nm stack thickens markedly during optimization whereas the total thickness of the 650nm stack only changes fractionally. The after-optimization 650nm stack is a much better uniform reflector, or silver mirror. Thickness are in micrometers and colours as figure 6.

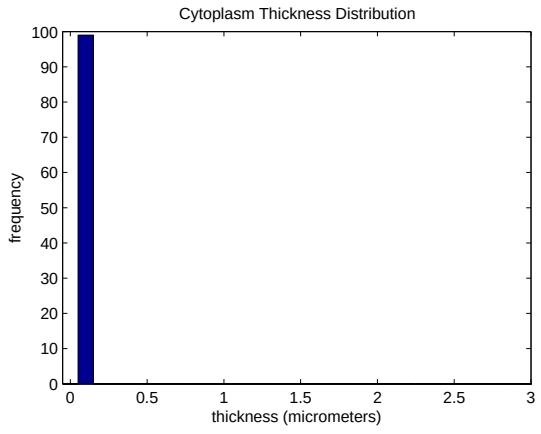

(a) Input thickness distribution of cytoplasm layers.

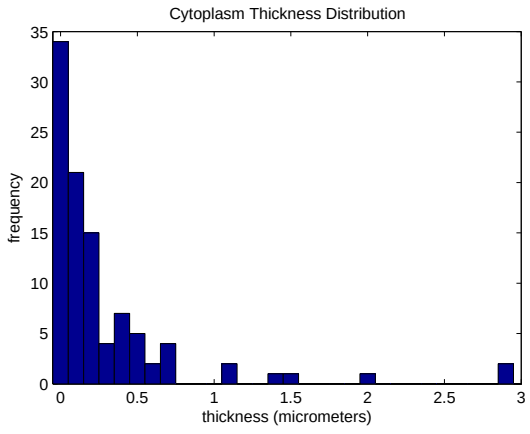

(b) Distribution of cytoplasm layer thicknesses after optimization.

Figure 10: Histograms of thicknesses of cytoplasm layers before and after optimization for the 550nm quarter wave stack. There is a large distortion of the distribution upon optimization as the stack grows and consequentially the thickness of cytoplasm layers increases.

3.6 Chirped and Double Chirped Stacks, 50 Layers, Fourth Deviates

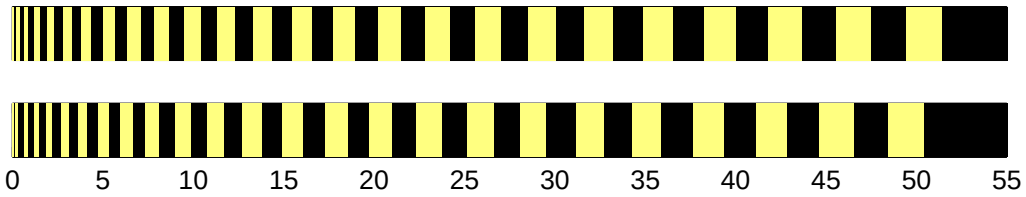

(a) Chirped stack with uniformly increasing layer thickness from 0.1 to 2μm. $f_4^{in} = 0.151$, $f_4^{out} = 0.0451$.

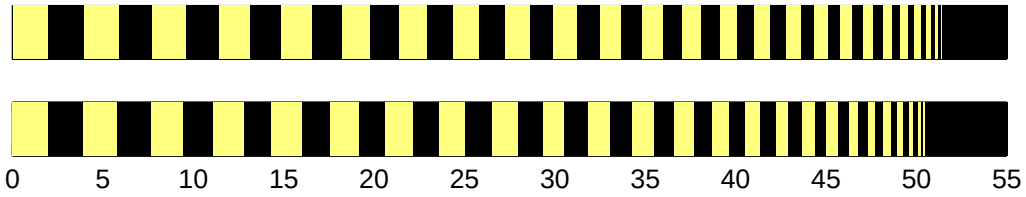

(b) Chirped stack with uniformly decreasing layer thickness from 2 to 0.1μm. $f_4^{in} = 0.151$, $f_4^{out} = 0.0435$.

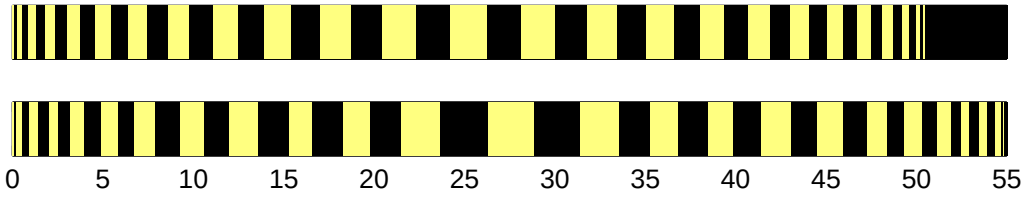

(c) Double chirped stack with thickness from 0.1 to 2 to 0.1μm. $f_4^{in} = 0.260$, $f_4^{out} = 0.0409$.

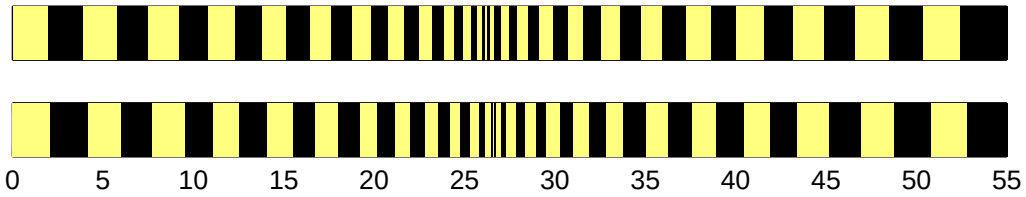

(d) Double chirped stack with thickness from 2 to 0.1 to 2μm. $f_4^{in} = 0.266$, $f_4^{out} = 0.0333$.

Figure 11: Diagrams of the 50 layer chirped stacks before and after optimization. It is clear from the renders that the optimization routine is getting stuck in a local minimum, as much of the chirped layer structure is preserved by the optimization.

Table 5 contains fourth moment optimizations for four chirped stacks of 50 layers. The chirped stacks all have input f-value $f_4^{in} \simeq 0.2$ which is comparable to the mean input f-value $\bar{f}_4^{in} = 0.153$ for the 50 layer random stacks. They have output f-value $f_4^{out} \simeq 0.04$ which is approximately five times small than the input f-value and again compares well with the mean output $\bar{f}_4^{out} = 0.0357$ f-value for the 50 layer random stacks. The results tentatively place chirped stacks on par with the random stacks, and shows they are significantly better silver reflectors than either the equal layer stacks or the quarter-wave stacks before optimization.

All the chirped stacks are depicted in figure 11. It is clear the optimization routine is halting in a local minimum of the f_4 value surface as none of the output stacks appear qualitatively different than the input chirped stacks apart from the layer thicknesses being distorted slightly. However this slight distortion does improve the f-value significantly.

Type Input Layer Thickness Profile	Chirped 0.1 to 2μm	Chirped 2 to 0.1μm	Double Chirped 0.1 to 2 to 0.1μm	Double Chirped 2 to 0.1 to 2μm
Input Total Thickness, h_T^{in} (μm)	51.45	51.45	50.5	52.4
Input f-value, f_4^{in}	0.151	0.151	0.260	0.266
Output f-value, f_4^{out}	0.0451	0.0435	0.0409	0.0333
Output Total Thickness, h_T^{out} (μm)	50.45	50.47	54.87	52.82

Table 5: Results for fourth moment chirped stack optimization runs, 50 layer stacks.

3.7 Quarter Wave Stack in Guanine, Random Cytoplasm Thickness, Optimizing Square Deviates

Wavelength (nm)	300	350	400	450	500	550
Input Total Thickness, h_T^{in} (μm)	39.35	38.53	38.50	39.14	37.65	41.53
Input Guanine, h_G^{in} (μm)	0.0408	0.0476	0.0543	0.0611	0.0679	0.0747
Input f-value, f_2^{in}	0.0436	0.0425	0.0274	0.0227	0.0255	0.0302
Output f-value, f_2^{out}	0.000449	0.0000136	0.0255	0.00673	0.000106	0.000400
Output Total Thickness, h_T^{out} (μm)	33.57	36.46	38.49	39.19	37.55	41.61
Output Mean Guanine, h_G^{out} (μm)	0.0510	0.0589	0.0543	0.0613	0.0681	0.0670
Output S.D. Guanine, $\sigma_{h_G^{out}}$ (μm)	0.0137	0.0190	0.00000548	0.000626	0.0872	0.0167
Output Mean Cytoplasm, h_C^{out} (μm)	0.288	0.309	0.334	0.334	0.311	0.353
Output S.D. Cytoplasm, $\sigma_{h_C^{out}}$ (μm)	0.277	0.272	0.306	0.277	0.283	0.312

Wavelength (nm)	600	650	700	750	800
Input Total Thickness (μm)	40.43	41.31	39.86	37.53	44.49
Input Guanine, h_G^{in} (μm)	0.0815	0.0883	0.0951	0.102	0.109
Input f-value, f_2^{in}	0.0773	0.111	0.130	0.138	0.138
Output f-value, f_2^{out}	0.00000869	0.000127	0.000492	0.00000538	0.0000146
Output Total Thickness (μm)	37.59	41.31	39.86	31.42	47.61
Output Mean Guanine, h_G^{out} (μm)	0.0641	0.0865	0.105	0.0719	0.109
Output S.D. Guanine, $\sigma_{h_G^{out}}$ (μm)	0.0178	0.0232	0.0768	0.0315	0.0613
Output Mean Cytoplasm, h_C^{out} (μm)	0.315	0.335	0.346	0.248	0.371
Output S.D. Cytoplasm, $\sigma_{h_C^{out}}$ (μm)	0.274	0.283	0.367	0.238	0.362

Table 6: Results for second moment guanine layer quarter-wave optimization runs, cytoplasm random in $[0, 1]$, 200 layer stacks.

In this final section of results, I examine the the quarter-wave stack of guanine only. This is where in the input stack the guanine layer thicknesses are all an optical quarter-wavelength and the cytoplasm thickness are chosen randomly. The results are presented in table 6.

The first thing of note is that these semi-random stacks on average have a five times lower input f-value f_2^{in} than either the equal layer or quarter-wave stacks. This supports the notion that variation in layer thicknesses is a requisite for uniform reflectivity. The average $f_2^{in} \simeq 0.1$ is greater than the 200 layer random input stacks and this may be because in effect half of the layers, namely the guanine layers, are redundant in helping to produce a silvery reflectance as they are only effective at reflecting one wavelength. An obvious and testable hypothesis would suggest that the mean second moment f-value for 100 layer random stacks is also about 0.1, as these stacks would have as much variation in layer thicknesses as the 200 layer guanine quarter-wave stacks.

The output stacks are structured akin to the results of the random stacks i.e. the output thickness is close to the input thickness and the distributions of cytoplasm layer thicknesses do not change much. Naturally

the guanine thickness distribution is different from its initial distribution however, with the output distribution generally being centered on the the initial guanine layer thickness with a small standard deviation.

4 Conclusion

The aim of this project was to learn more about how guanine cytoplasm bi-layers can be manufactured to reflect visible light uniformly across the spectrum. This is a relevant topic for explaining how fish can camouflage themselves against the silvery surface of water. I developed a method to measure likeness of two spectra as a number in the range $[0, 1]$; the lower the number, the "closer" the two spectra are to each other. The method can be calibrated to favour spectra which are more alike in terms of mean reflectivity (lower moments), or with fewer disparate reflectivities hence more alike in colour (higher moments).

In the methods section I used electromagnetic and optical theory to devise a simple model for the reflectivity of a bi-layer stack and stated any assumptions. I identified the variables on which the reflectivity of the stack is dependent. In effect for the fish trying to camouflage itself, the parameters under its control in the simple model are the number of layers in the stack and the thicknesses of the layers (with a limitation on the total thickness of the stack). I investigate solution stacks which minimize f-value relative to a unity "silver mirror" spectrum by varying these parameters. A MATLAB numerical optimization routine is used to find local solutions of the f-value surface defined by the layer thicknesses.

The first result to conclude is that the number of layers in the stack is the easiest way to control the reflectivity of a stack. I show that for randomly initialized stacks with layer thicknesses of the same order of magnitude as the wavelengths of visible light that increasing the number of layers will guarantee a reduction in f-value. The optimization routine demonstrates that adjusting layer thicknesses in a random stack is only likely to lead to one of many degenerate local solutions. There is no simple rule to indicate which adjustments to make and the result is extremely sensitive to slight errors in thicknesses due to the pitted nature of the f-value surface.

Basic stack geometries such as equal layer stacks and quarter-wave stacks are found to be poor uniform reflectors. In most cases the optimization algorithm succeeds in reducing the f-values of these stacks in line with the random stacks, and where appropriate the chirped stacks (50 layer quarter-wave stack results in appendix §A.2). This is evidence that variation in layer thicknesses is key for uniform reflectance.

I show that by transforming a quarter-wave stack into a quarter-wave stack for guanine only, random cytoplasm layer thicknesses, that the reflectivity of the stack improves and predict that this operation will bring the f-value in line with a random stack with half the number of layers. This provides further evidence that quarter-wave stacks are poor solutions in comparison to the stacks with variations in layer thicknesses. It is natural to extend my analysis to include initial stacks which are superpositions of quarter-wave stacks for many wavelengths. It seems unlikely given the evidence I present that such a stack would be any better in terms of f-value than one of the chirped or random in ital stacks as there would be lower variation in the layer thicknesses.

5 Extensions

Throughout the course of this research many questions were put forward by my supervisors and I to try and gain a deeper understanding of how a silvery camouflage mechanism works. Here I discuss the questions which fall naturally into three stands. Firstly I scrutinize the simplifications and assumptions of my model and how they may affect the predictions made. Secondly I discuss some engineering constraints on how fish grow guanine-cytoplasm bi-layers within their skin. And finally thoughts turn to the predators of the silvery fish and question how good the camouflage needs to be to counter this threat.

An initial assumption of the model was that guanine and cytoplasm are both isotropic, non-absorbing and non-magnetic materials. The last assumption is almost certainly true, perhaps to the extent that the predictions are accurate to many orders of magnitude. Cytoplasm is a fluid with a disordered structure meaning it should be isotropic, however it is likely to absorb a small fraction of light particularly at wavelengths which excite the constituent molecules of the mixture. Guanine is a crystal structured as rhombic platelets of multiple layers of molecules. The crystal structure is likely to lead to a directional dependence of its optical properties, and the direction in which the platelets are arranged relative to the crystals suspended in the cytoplasm is likely to the be the biggest source of error in the model. Guanine is highly transparent but will still absorb a fraction of propagating visible light. Accounting firstly for the anisotropic nature of guanine then a degree of absorption

of the materials in an extended model would be a good way to validate or establish weaknesses in the model presented here.

Also assumed in my model was that the layers in the skin are perfectly flat and parallel. As can been seen from the electron micrograph of a cross section of fish skin in figure 1 of the introduction, the guanine crystals are in fact suspended in a continuous fluid of cytoplasm. This means that neither of the assumptions are universally true for all fish, and the literature shows different constructions of guanine-cytoplasm stacks in different species (Kinoshita and Yoshioka [2005] and Parker [2000]). The geometry of the layers in figure 1 makes finding an analytic solution to the reflectivity hard, and it might be easier to examine superpositions of spectra for stacks with similar geometry but variation in the positions of boundaries to try understand how this structure affects the overall reflectivity. It may be possible that the structure of the stack with non-parallel layers may add the variation into the optical paths which I conclude is vital for a silvery reflectance in my conclusions.

I established that the optimization process was terminating in a local minima of the f-value surface. There are two strands to this problem: firstly I noted that the settings of the optimization routine may need tweaking, and secondly that there are many almost degenerate solutions of assembling a silvery bi-layer stacks. The latter issue is discussed in the following notes on the engineering of a stack in a fish skin and the capabilities of the predator. I ask is the global solution feasible in terms of construction? And then is it necessary or are other solutions sufficient? Finally the optimization process fails to account for different angles of incidence of light on the stack and research is needed into the effect it has on the conclusions drawn.

In terms of the construction of a bi-layer in fish skin, the following points are noted. When the optimization routine suggests that sub-micrometer adjustments to layer thicknesses may dramatically improve the silvery reflectance of the stack, I ask how accurately can a fish assemble guanine layers, what is the minimum thickness the layers can be made, and how flat are the layers. I also question how robust the structure is: do the optical thicknesses of the layers change as a fish bends and flexes its scales by swimming and breathing. It would be unrealistic to assume a fish can spent lots of resources constructing precision optical instruments only for an elementary process of life to change the structure and destroy any gains. It is for this reason McKenzie et al. [1995] suggests that the chaotic or random structure of layers is best, as it is robust to error and change.

It would be interesting to consider different functions minimized in the optimization routine. Would it be more appropriate to devise a function which favours a flat reflectance spectrum above a spectrum with high mean reflectivity. This is the same as asking is a slightly duller but silver reflectance better than a brighter but slightly coloured reflectance. This question could depend on the light conditions and the nature of the surface of the water. Another function to consider could be one which places a cost to the total volume of guanine used in the structure, as guanine is an expensive resource for the fish to machine.

When considering a form of camouflage it is appropriate to ask what the predator is able to see. Can different predators see different regions and contrasts in the visible spectrum better than others? And what is the resolution that the predator can distinguish? These questions have consequences for how good the camouflage needs to be, and ultimately how much resource has to be invested in the manufacture of the bi-layer stacks.

A Supplementary Results

A.1 Quarter Wave Stack, 200 Layers, Second Deviates, Additional Renders

Figures 12 and 13 are the additional renders of the second moment 200 layer quarter-wave stacks of table 4 in §3.5.

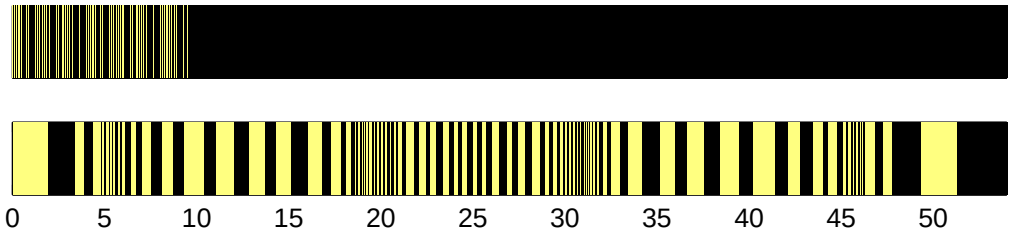

(a) 300nm quarter-wave stack. $f_2^{in} = 0.848,\ f_2^{out} = 0.000165.$

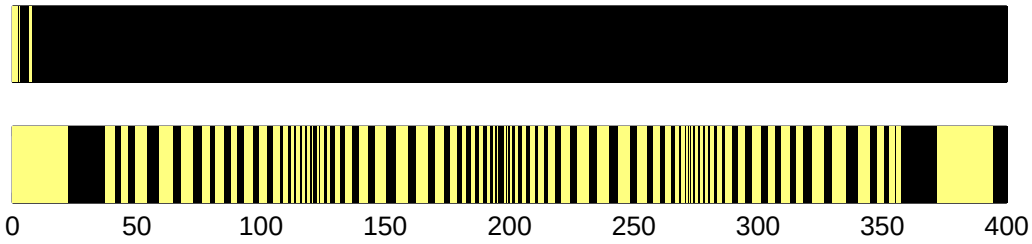

(b) 350nm quarter-wave stack. $f_2^{in} = 0.748,\ f_2^{out} = 0.0948.$

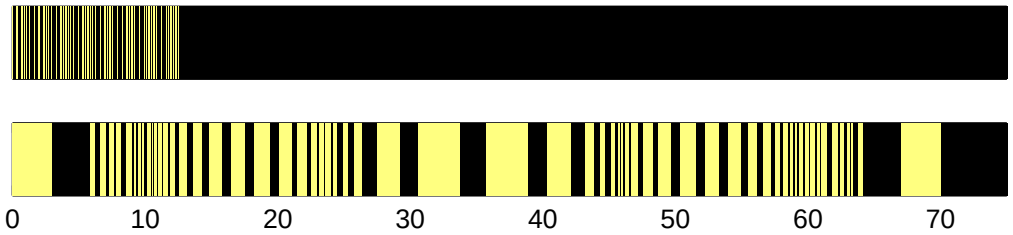

(c) 400nm quarter-wave stack. $f_2^{in} = 0.708,\ f_2^{out} = 0.0555.$

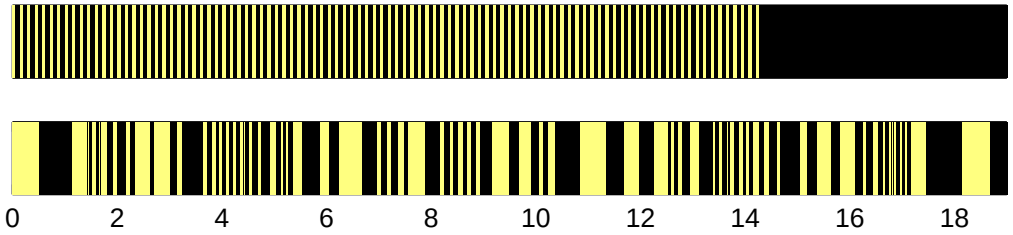

(d) 450nm quarter-wave stack. Fractional change in output stack thickness. $f_2^{in} = 0.674,\ f_2^{out} = 0.000372.$

Figure 12: Part 1 of additional 200 layer quarter-wave stack renders. Part 2 overleaf. Before and after optimization f-values stated in captions. Thicknesses to scale and measured in micrometers.

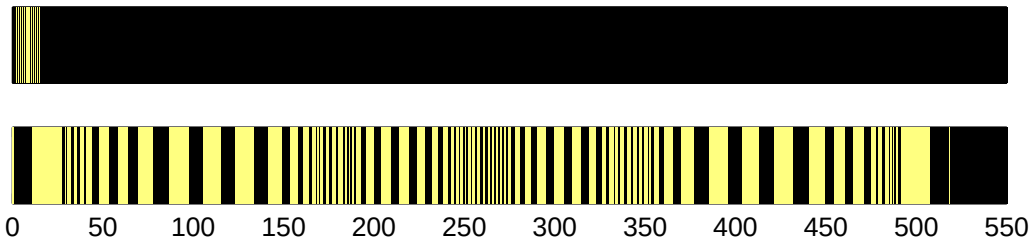

(a) 500nm quarter-wave stack. $f_2^{in} = 0.647$, $f_2^{out} = 0.0801$.

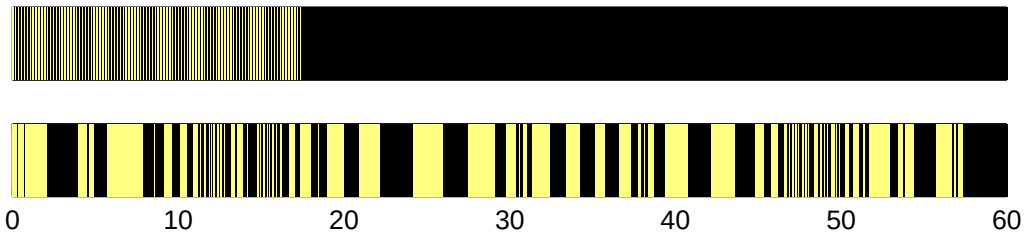

(b) 550nm quarter-wave stack. $f_2^{in} = 0.625$, $f_2^{out} = 0.000159$.

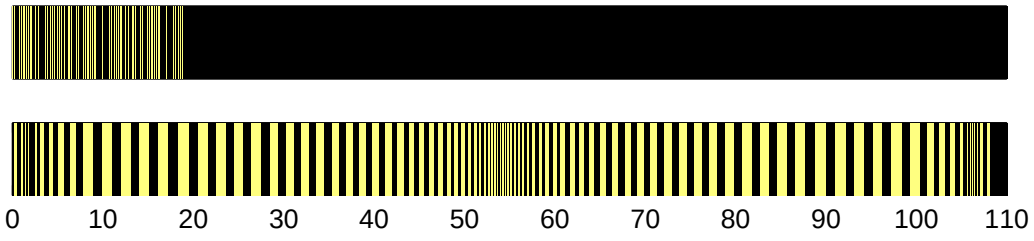

(c) 600nm quarter-wave stack. $f_2^{in} = 0.609$, $f_2^{out} = 0.101$.

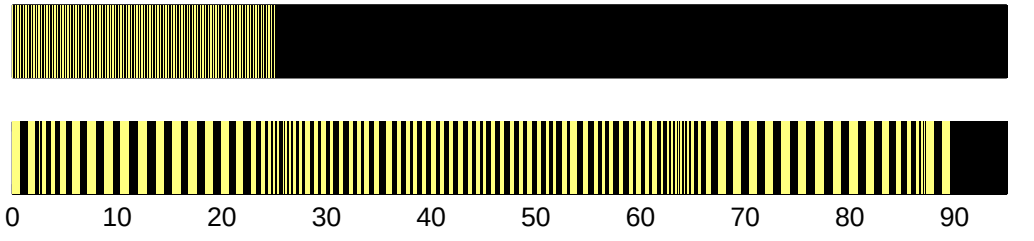

(d) 750nm quarter-wave stack. $f_2^{in} = 0.677$, $f_2^{out} = 0.0327$.

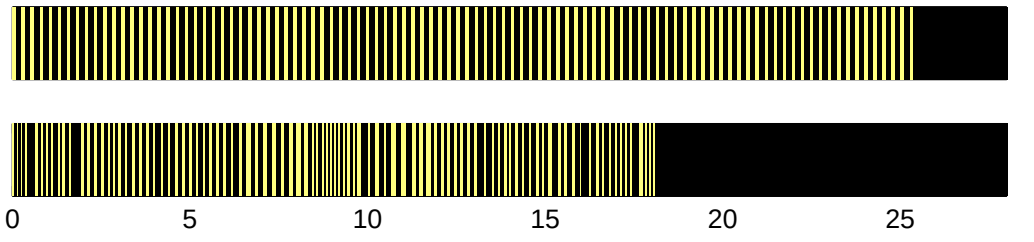

(e) 800nm quarter-wave stack. Fractional change in output stack thickness. $f_2^{in} = 0.759$, $f_2^{out} = 0.00000850$.

Figure 13: Part 2 of additional quarter-wave stack renders. Before and after optimization f-values stated in captions. Thicknesses to scale and measured in micrometers.

A.2 Quarter Wave Stack, 50 Layers, Fourth Deviates

Wavelength (nm)	400	600	800
Input Total Thickness, h_T^{in} (μm)	3.12	4.68	6.23
Input Guanine, h_G^{in} (μm)	0.0543	0.0815	0.109
Input f-value, f_4^{in}	0.694	0.422	0.648
Output f-value, f_4^{out}	0.000359	0.0103	0.00390
Output Total Thickness, h_T^{out} (μm)	3.74	22.00	6.74
Output Mean Guanine, h_G^{out} (μm)	0.0685	0.428	0.101
Output S.D. Guanine, $\sigma_{h_G^{out}}$ (μm)	0.0415	0.495	0.0516
Output Mean Cytoplasm, h_C^{out} (μm)	0.0845	0.471	0.176
Output S.D. Cytoplasm, $\sigma_{h_C^{out}}$ (μm)	0.0455	0.762	0.0812

Table 7: Results for fourth moment quarter-wave optimization runs, 50 layer stacks.

Additional results showing three quarter-wave stack optimizations of 50 layer stacks using fourth deviates. The results are similar to the 200 layer second moment quarter-wave stack optimizations of §3.5.

1. All input quarter-wave stacks are poor uniform reflectors with $f_4^{in} \simeq 0.5$. The random input stacks have $\bar{f}_4^{in} = 0.153$ and are better uniform reflectors (§3.3).

2. The 600nm quarter-wave stack thickens upon optimization, and the improvement in f-value is a reduction by factor 40. The output f-value $f_4^{out} = 0.0103$ is in line with $\bar{f}_4^{out} = 0.0656$ of the random stacks and $f_4^{out} \simeq 0.04$ of the chirped stacks.

3. The 400nm and 600nm quarter-wave stacks only fractionally different than the output stacks in total thickness. Their f_4^{out} f-values compare favourably with the random stack optimization runs.

4. All optimized quarter-wave stacks have a variation of layer thicknesses, $\sigma_{h_G^{out}} \sim \sigma_{h_C^{out}} \sim 0.1\mu$m.

B Code

B.1 basicmodel.m - Reflectivity and Transmissivity prediction

```
% basicmodel.m
% 6th December 2008 - Alex Malins
% Predict reflectivity and transmissivity of a stratified stack of isotropic
% non-magnetic dielectric films.

% input variables
N=2;   % number of layers in the stack
n=[1.84, 1.365];  % vector of refractive indices of layers
n_F=1.365; % refractive index of first semiinfinite medium
n_L=1.365; % refractive index of last semiinfinite medium
h=[0.25, 0.25] % vector of thicknessess of layers (microns)
lambda=0.4:0.001:0.8; % vector of wavelengths of incident light (microns)
theta_min=0; % range of angles of incidence of light (radians)
theta_increment=(pi/180);
theta_max=(pi/2);

no_theta=floor((theta_max-theta_min)/theta_increment)+1;
theta=zeros(N+2,no_theta);
theta(1,:)=theta_min:theta_increment:theta_max;
thetadegrees=180/pi*theta;

for j=1:no_theta,   % theta for first layer
    novern=n_F/n(1);
    theta(2,j)=asin(novern*sin(theta(1,j)));
end
for i=2:N,    % loop over all layers bar first
    novern=n(i-1)/n(i);
    for j=1:no_theta, % theta for i'th layer
        theta(i+1,j)=asin(novern*sin(theta(i,j)));
    end
end
for j=1:no_theta,   % theta for last semiinfinite medium
    novern=n(N)/n_L;
    theta(N+2,j)=asin(novern*sin(theta(N+1,j)));
end

lambdananano=1000*lambda; % wavelength vector (nanometers)
k_1=2*pi./lambda; % wavenumber vector (microns^-1)

for k=1:length(k_1),    % loop through wavenumber vector
    for j=1:no_theta,   % loop through theta vector
        M_TE_i=eye(2); % reset 2x2 "M" matricies to identity
        M_TE=eye(2);
        M_TM_i=eye(2);
        M_TM=eye(2);
        for i=1:N,    % loop over all layers
            n_icostheta_ij=n(i)*cos(theta(i+1,j));
            k_1n_ih_icostheta_ij=k_1(k)*h(i)*n_icostheta_ij;

            %M_TE_i characteristic matrix for i'th layer, TE wave
```

```
51              M_TE_i(1,1)=cos(k_1n_ih_icostheta_ij);
52              M_TE_i(1,2)=0-sqrt(-1)*sin(k_1n_ih_icostheta_ij)/n_icostheta_ij;
53              M_TE_i(2,1)=0-sqrt(-1)*sin(k_1n_ih_icostheta_ij)*n_icostheta_ij;
54              M_TE_i(2,2)=cos(k_1n_ih_icostheta_ij);
55              M_TE=M_TE*M_TE_i;
56
57              %M_TM_i characteristic matrix for i'th layer, TM wave
58              invn_icostheta_ij=cos(theta(i+1,j))/n(i);
59              M_TM_i(1,1)=cos(k_1n_ih_icostheta_ij);
60              M_TM_i(1,2)=0-sqrt(-1)*sin(k_1n_ih_icostheta_ij)/invn_icostheta_ij;
61              M_TM_i(2,1)=0-sqrt(-1)*sin(k_1n_ih_icostheta_ij)*invn_icostheta_ij;
62              M_TM_i(2,2)=cos(k_1n_ih_icostheta_ij);
63              M_TM=M_TM*M_TM_i;
64          end
65          n_Fcostheta_Fj=n_F*cos(theta(1,j));
66          n_Lcostheta_Lj=n_L*cos(theta(N+2,j));
67          A1_TE(k,j)=0.5*(M_TE(1,1)+M_TE(1,2)*n_Lcostheta_Lj
68                          +(M_TE(2,1)+M_TE(2,2)*n_Lcostheta_Lj)/n_Fcostheta_Fj);
69          B1_TE(k,j)=0.5*(M_TE(1,1)+M_TE(1,2)*n_Lcostheta_Lj
70                          -(M_TE(2,1)+M_TE(2,2)*n_Lcostheta_Lj)/n_Fcostheta_Fj);
71          absA1_TE_square=abs(A1_TE(k,j))^2;
72          absB1_TE_square=abs(B1_TE(k,j))^2;
73          R_TE(k,j)=absB1_TE_square/absA1_TE_square;
74          T_TE(k,j)=n_Lcostheta_Lj/(n_Fcostheta_Fj*absA1_TE_square);
75          err_TE(k,j)=n_Fcostheta_Fj*(absA1_TE_square-absB1_TE_square)-n_Lcostheta_Lj;
76
77          invn_Fcostheta_Fj=cos(theta(1,j))/n_F;
78          invn_Lcostheta_Lj=cos(theta(N+2,j))/n_L;
79          A1_TM(k,j)=0.5*(M_TM(1,1)+M_TM(1,2)*invn_Lcostheta_Lj
80                          +(M_TM(2,1)+M_TM(2,2)*invn_Lcostheta_Lj)/invn_Fcostheta_Fj);
81          B1_TM(k,j)=0.5*(M_TM(1,1)+M_TM(1,2)*invn_Lcostheta_Lj
82                          -(M_TM(2,1)+M_TM(2,2)*invn_Lcostheta_Lj)/invn_Fcostheta_Fj);
83          absA1_TM_square=abs(A1_TM(k,j))^2;
84          absB1_TM_square=abs(B1_TM(k,j))^2;
85          R_TM(k,j)=absB1_TM_square/absA1_TM_square;
86          T_TM(k,j)=invn_Lcostheta_Lj/(invn_Fcostheta_Fj*absA1_TM_square);
87          err_TM(k,j)=invn_Fcostheta_Fj*(absA1_TM_square-absB1_TM_square)-invn_Lcostheta_Lj;
88      end
89  end
```

B.2 `stacksquaredresiduals.m` - Calculation of mean square deviates

```
% stacksquareresiduals.m
% 6th December 2008 - Alex Malins
% Calculate squared residual deviates from desired spectrum for normal
% incident plane light on a multilayer stack.
% Input N-1 sqrt layer thicknesses.

function fvalue = stacksquareresiduals(root2h)

% Variables
[speclambda,specR]=textread('spectrum.z','%f %f'); % read desired spectrum
N=200; % number of layers
n_F = 1.365;
n_G = 1.84; % guanine refractive index
n_C = 1.365;    % cyctoplasm refractive index
n_L = 1.365;
stackthickness=2000; % total stack thickness
lambda=0.3:0.001:0.8; % vector of wavelengths of incident light (microns)

h_N=0;
for i=1:1:N-1,
    h(i)=root2h(i)*root2h(i);   % i'th layer thickness
    h_N=h_N+h(i);
end
h_N=stackthickness-h_N; % N'th layer thickness

for i=1:1:N/2,
    n(2*i)=n_C;
    n(2*i-1)=n_G;
end

lambdanano=1000*lambda; % wavelength vector (nanometers)
k_1=2*pi./lambda; % wavenumber vector (microns^-1)

residerror=0;
for k=1:length(k_1),    % loop through all wavenumbers
    M_TE_i=eye(2);
    M_TE=eye(2);
    for i=1:N,    % loop over all layers
        if (i==N),
            k_1n_ih_i=k_1(k)*h_N*n(i);
        else
            k_1n_ih_i=k_1(k)*h(i)*n(i);
        end

        M_TE_i(1,1)=cos(k_1n_ih_i);
        M_TE_i(1,2)=0-sqrt(-1)*sin(k_1n_ih_i)/n(i);
        M_TE_i(2,1)=0-sqrt(-1)*sin(k_1n_ih_i)*n(i);
        M_TE_i(2,2)=cos(k_1n_ih_i);
        M_TE=M_TE*M_TE_i;
    end
    A1_TE(k)=0.5*(M_TE(1,1)+M_TE(1,2)*n_L+(M_TE(2,1)+M_TE(2,2)*n_L)/n_F);
    B1_TE(k)=0.5*(M_TE(1,1)+M_TE(1,2)*n_L-(M_TE(2,1)+M_TE(2,2)*n_L)/n_F);
```

```
53        absA1_TE_square=abs(A1_TE(k))^2;
54        absB1_TE_square=abs(B1_TE(k))^2;
55        R_TE(k)=absB1_TE_square/absA1_TE_square;
56        residerror=residerror+(R_TE(k)-specR(k))^2; % f-value moment is exponent here
57    end
58    fvalue=residerror/(length(k_1));
```

References

F. Abelès. Recherches sur la propagation des ondes électromagnetiques sinusoidales dans les milieus stratifiés. *Ann. Phys. (Paris)*, 5:596–640 and 706–784, 1950.

Max Born and Emil Wolf. *Principles of Optics 7th (expanded) edition*. Cambridge University Press, 1999.

C. G. Broyden. The convergence of a class of double-rank minimization algorithms. *Journal Inst. Math. Applic.*, 6:79–90, 1970.

E. J. Denton and M. F. Land. Mechanism of reflexion in silvery layers of fish and cephalopods. *Proceedings of the Royal Society of London. Series B, Biological Sciences*, 178(1050):43–61, 1971. ISSN 00804649. URL `http://www.jstor.org/stable/75954`.

E. J. Denton and J. A. C. Nicol. Polarization of light reflected from the silvery exterior of the bleak alburnus alburnus. *J. Mar. Bio. Assoc. UK*, 45:711, 1965.

R. Fletcher. *Practical Methods of Optimization*. John Wiley and Sons, 1980.

A. F. Huxley. A theoretical treatment of the reflexion of light by multilayer structures. *J Exp Biol*, 48(2):227–245, 1968. URL `http://jeb.biologists.org/cgi/content/abstract/48/2/227`.

Shuichi Kinoshita and Shinya Yoshioka. Structural colors in nature: The role of regularity and irregularity in the structure. *ChemPhysChem*, 6(8):1442–1459, 2005. URL `http://dx.doi.org/10.1002/cphc.200500007`.

J. N. Lythgoe, Julia Shand, and R. G. Foster. Visual pigment in fish iridocytes. *Nature*, 308(5954):83–84, March 1984. URL `http://dx.doi.org/10.1038/308083a0`.

H. A. Macleod. *Thin Film Optical Filters Second Edition*. Adam Hilger Ltd, 1986.

C. Martijn de Sterke and R. C. McPhedran. Bragg remnants in stratified random media. *Phys. Rev. B*, 47(13): 7780–7787, Apr 1993. doi: 10.1103/PhysRevB.47.7780.

David R. McKenzie, Yongbai Yin, and William D. McFall. Silvery fish skin as an example of a chaotic reflector. *Proceedings: Mathematical and Physical Sciences*, 451(1943):579–584, 1995. ISSN 09628444. URL `http://www.jstor.org/stable/52739`.

Andrew R. Parker. 515 million years of structural colour. *Journal of Optics A: Pure and Applied Optics*, 2(6): R15–R28, 2000. URL `http://stacks.iop.org/1464-4258/2/R15`.

K. M. Yoo and R. R. Alfano. Broad bandwidth mirror with random layer thicknesses. *Appl. Opt.*, 28(13): 2456–2458, 1989. URL `http://ao.osa.org/abstract.cfm?URI=ao-28-13-2456`.